

Equation of state for strongly interacting matter: collective effects, Landau damping and predictions for LHC

R. Schulze[†], M. Bluhm, B. Kämpfer

Forschungszentrum Dresden-Rossendorf, PF 510119, 01314 Dresden, Germany
 Institut für Theoretische Physik, TU Dresden, 01062 Dresden, Germany

Abstract

The equation of state (EOS) is of utmost importance for the description of the hydrodynamic phase of strongly interacting matter in relativistic heavy-ion collisions. Lattice QCD can provide useful information on the EOS, mainly for small net baryon densities. The QCD quasiparticle model provides a means to map lattice QCD results into regions relevant for a variety of experiments. We report here on effects of collective modes and damping on the EOS. Some predictions for forthcoming heavy-ion collisions at LHC/ALICE are presented and perspectives for deriving an EOS for FAIR/CBM are discussed.

1 Introduction

The equation of state (EOS) for strongly interacting matter is needed as input for hydrodynamical calculations of the expanding fireball created in relativistic heavy-ion collisions (HIC). Theoretical predictions (cf. [1] for a survey) and recent experimental results [2–5] point to a transition from confined hadronic matter to the quark-gluon plasma (QGP), being a new deconfined state which is governed by the fundamental quark and gluon degrees of freedom. That means, a usable EOS has to uncover both states.

Upcoming HIC experiments at LHC, mainly to be investigated by ALICE, will probe the high-temperature region at small net baryon densities, while the future HIC experiments at FAIR, to be addressed by CBM, are aimed at exploring the region of high net baryon densities. Therefore, the EOS in a wide region of the phase diagram is needed. Numerical simulations of QCD on the lattice are still constrained to small net baryon densities. Consequently, there is a need for phenomenological models which allow predictions in regions of the phase diagram not yet accessible by lattice QCD calculations. Here we discuss a phenomenological model which relies on the picture of quarks and gluons as non-interacting quasiparticle excitations. The employed quasiparticle model (QPM) goes back to [6–10], while recent work has been presented in [11–16]. Alternative formulations have been given, e.g., in [17, 18].

2 The quasiparticle model

The description of strongly interacting matter is governed by QCD. Thus the foundation of any model has to be the quantized Lagrangian \mathcal{L}_{QCD} and the dressed propagators and full self-energies obtained from it. In the framework of finite-temperature field theory a thermodynamical potential Ω can be derived using

[†]r.schulze@fzd.de, invited talk given at XLVI International Winter Meeting on Nuclear Physics in Bormio, Italy, 20–26 Jan 2008

the Cornwall-Jackiw-Tomboulis (CJT) formalism [19]. It employs the effective action

$$\begin{aligned}\Gamma[D, S] = & I - \frac{1}{2} \{ \text{Tr} [\ln D^{-1}] + \text{Tr} [D_0^{-1} D - 1] \} \\ & + \{ \text{Tr} [\ln S^{-1}] + \text{Tr} [S_0^{-1} S - 1] \} + \Gamma_2[D, S],\end{aligned}\quad (1)$$

where I is the classical action containing \mathcal{L}_{QCD} , and D and S are the dressed gluon and quark propagators (the subscript 0 denotes the respective free equivalents). The functional Γ_2 represents the sum over all two-particle irreducible skeleton graphs of the theory, i.e. all those graphs without external lines that do not fall apart upon cutting of two propagators.

For translationally invariant systems without broken symmetries the expression (1) simplifies and gives the thermodynamic potential at finite temperature T [16]

$$\begin{aligned}\frac{\Omega}{V} = & \text{tr} \int \frac{d^4 k}{(2\pi)^4} n_B(\omega) \text{Im}(\ln D^{-1} - \Pi D) \\ & + 2 \text{tr} \int \frac{d^4 k}{(2\pi)^4} n_F(\omega) \text{Im}(\ln S^{-1} - \Sigma S) - \frac{T}{V} \Gamma_2,\end{aligned}\quad (2)$$

where Π and Σ are the full self-energies of gluons and quarks respectively. Truncating Γ_2 at 2-loop order leaving

$$\Gamma_2 = \frac{1}{12} \text{diagram}_1 + \frac{1}{8} \text{diagram}_2 - \frac{1}{2} \text{diagram}_3 \quad (3)$$

directly leads to the well-known 1-loop quark and gluon self-energies [20]. Assuming additionally small external momenta or, equivalently, hard thermal loops ensures gauge invariance. These approximations are used in what follows.

An important quantity of the strong interaction and consequently also of our model is the running coupling g^2 which depends on the ratio of renormalization scale and QCD scale parameters. In order to phenomenologically accommodate higher-order and even non-perturbative effects of QCD we replace the former at $\mu = 0$ (μ is the quark chemical potential) by the first Matsubara frequency $i\pi T$ and shift the temperature T by a parameter T_s . The new quantity corresponds to an effective coupling and is denoted by G^2 (see [14] for details):

$$G^2(T \geq T_c, \mu = 0) = \frac{16\pi^2}{\beta_0 \ln x^2} \left(1 - \frac{4\beta_1}{\beta_0^2} \frac{\ln[\ln x^2]}{\ln x^2} \right), \quad (4)$$

where $x \equiv \lambda(T - T_s)/T_c$.

From the resulting thermodynamic potential we find the entropy density $s := -V^{-1} \partial\Omega/\partial T|_\mu = s_{g,T} + s_{g,L} + \sum_{q,s} (s_{i,\text{Pt.}+} + s_{i,\text{Pl.}})$ as a sum of four seemingly non-interacting quasiparticle families. Transverse gluons (g,T) and the quark particle ($i,\text{Pt.}$) contributions have a real particle interpretation while longitudinal gluons (plasmons, g,L) and the quark plasmino ($i,\text{Pl.}$) contributions are collective modes similar to phonons in solid state physics.

Although no obvious interaction terms appear within the one-loop entropy density, quark-gluon interactions are incorporated via damping terms as part of the single quasiparticle contributions. For instance, the transverse gluon entropy density reads

$$s_{g,T} = +2d_g \int \frac{d^4 k}{(2\pi)^4} \frac{\partial n_B}{\partial T} \left\{ \pi \varepsilon(\omega) \Theta(-\text{Re} D_T^{-1}) - \arctan \frac{\text{Im} \Pi_T}{\text{Re} D_T^{-1}} + \text{Re} D_T \text{Im} \Pi_T \right\}, \quad (5)$$

where the first term represents the real quasiparticle entropy density being equal to the entropy density of an ideal gas but with an implicit dispersion relation $\omega^2 = k^2 + \Pi_i(\omega, k)$, where $\Pi_i(\omega, k)$ are the respective self-energies of species i which depend furthermore on temperature and chemical potential. The second and third terms represent the Landau damping.

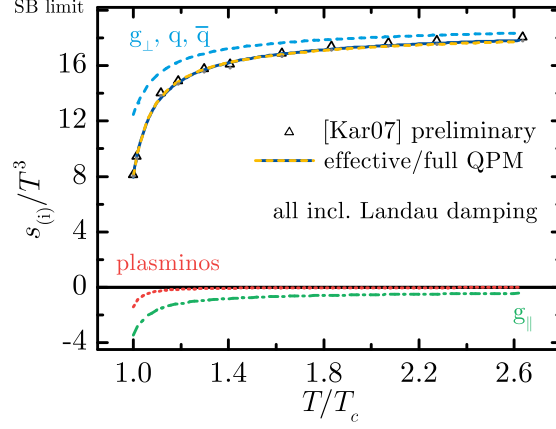


Figure 1: Adjustment of both full (solid line, $T_s = -0.73T_c$ and $\lambda = 6.1$) and effective (dashes on solid line, $T_s = -0.75T_c$ and $\lambda = 6.3$) QPMs to lattice data for the entropy density s/T^3 from [21] (continuum extrapolated by a factor of 0.96). Contributions to the full QPM are given by the dashed (transverse gluons, quarks, antiquarks), dotted (plasminos) and dash-dotted (plasmons) lines.

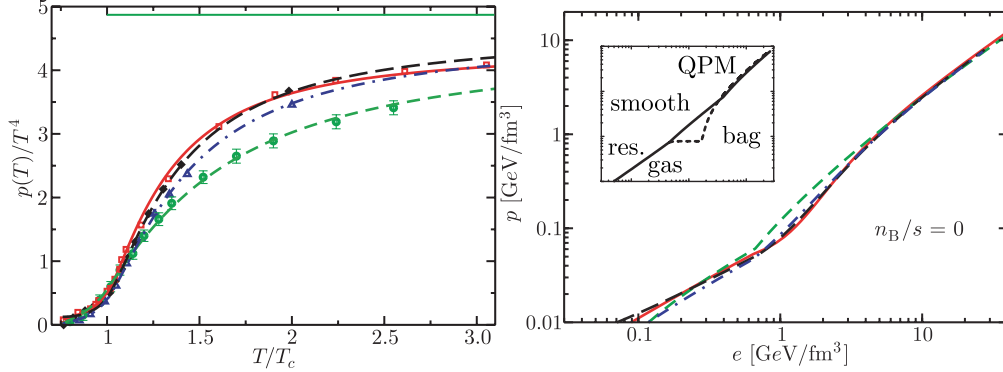


Figure 2: Left panel: Adjustments of the scaled eQP pressure p/T^4 to various lattice calculations (Ref. [22] - squares, Ref. [23] - diamonds and triangles, Ref. [24] - circles). Right panel: Corresponding EOS in the form of pressure p as a function of energy density e . For details see [15].

At zero chemical potential μ , both damping terms and the plasmon and plasmino entropies give only small contributions. Omitting those, an effective quasiparticle model (eQP) can be formulated to simplify the description/prediction of experiments with negligibly small net baryon density. This is a good approximation, e.g., for Au+Au collisions at RHIC or Pb+Pb collisions at LHC. Also note that the eQP uses the asymptotic approximation of the dispersion relation near the light cone, $\omega^2 = k^2 + m_{i,\infty}^2$, with $m_{i,\infty}$ as asymptotic quasiparticle masses which depend on T and μ both explicitly and implicitly (via G^2).

3 EOS for $\mu \approx 0$

In order to obtain sensible predictions, the QPM is adjusted to lattice data. Exploring the flexibility of the QPM introduced by the effective coupling we find excellent agreement of both the full QPM and the effective QPM with lattice data, see Figs. 1 and 2. In light of the substantially more involved nature of the full QPM it is very notable that both models give essentially the same good description of available lattice data. Fig. 1 also shows that plasmons and plasminos give negative contributions to the entropy

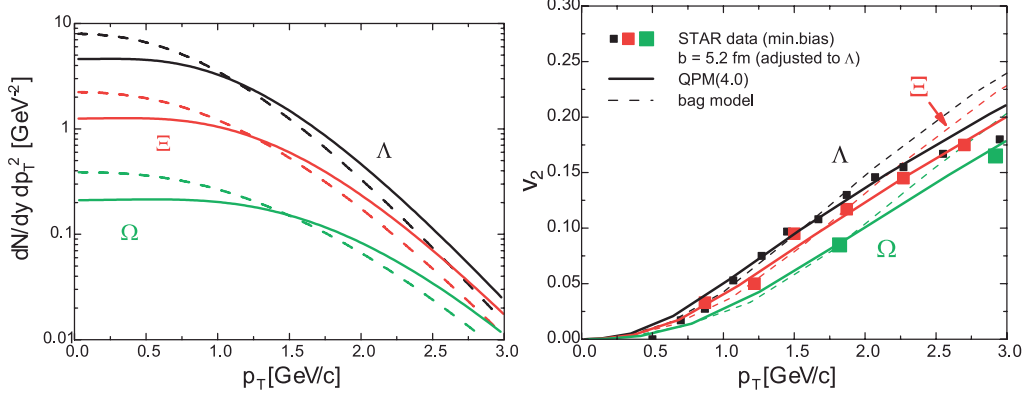


Figure 3: Transverse momentum spectra (left) and azimuthal distribution v_2 of emitted hadrons (right) for some strange baryons. Symbols represent experimental data [25] for Au+Au collisions at RHIC. For details see [15].

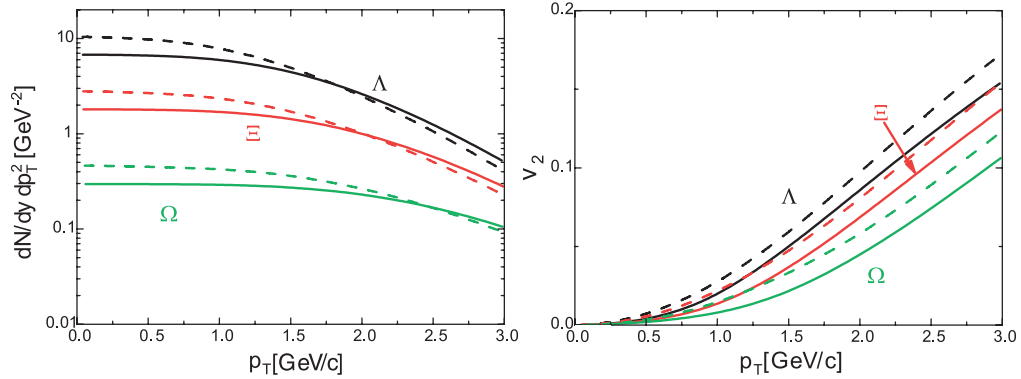


Figure 4: Transverse momentum spectra (left) and azimuthal distribution of emitted hadrons v_2 (right) for the same particles as in Figure 3 as predicted for Pb+Pb collisions at LHC. For details see [15].

density which is due to correlations introduced into the quark-gluon system by those collective modes.

It is remarkable that even though there still are substantial difference between various lattice QCD results, which are e.g. due to the used actions, lattice sizes and continuum extrapolations, the QPM EOS in the form $p(e)$ is unique above a threshold of about $e \gtrsim 4 \text{ GeV/fm}^3$ (Fig. 2). Some uncertainty is seen in the regions of lower energy densities. We suppose that the hadron resonance gas is the correct description of strongly interacting matter in the confined region. In order to examine the impact of this uncertainty we investigate two extreme cases: (i) a smooth crossover (labeled “QPM 4.0”), and (ii) a first order transition between resonance gas and the confident region of our QPM (labeled “bag model”).

To do so we use a relativistic hydrodynamic model to simulate Au+Au collisions at RHIC energies. Fig. 3 shows the resulting transverse momentum spectra and the azimuthal anisotropy coefficient v_2 of the baryons Λ , Ξ and Ω for an initial state characterized by $s_0 = 110 \text{ fm}^{-3}$ and initial proper time $\tau_0 = 0.6 \text{ fm/c}$. The latter is compared to actual experimental results [25], showing good agreement of both crossover and first order phase transition in the transverse momentum region $p_T \lesssim 1.8 \text{ GeV}$ considered relevant for hydrodynamics. Above this region, a simple crossover from the resonance gas to the QPM clearly provides better description of the measured data.

To consider Pb+Pb collisions at LHC, a conservative guess can give first indications of possible differences to RHIC. LHC particle yields are assumed to be three times larger than at RHIC, hinting to $s_0^{\text{LHC}} = 3s_0^{\text{RHIC}} = 330 \text{ fm}^{-3}$ ($T_0 = 515 \text{ MeV}$) with the assumption of $\tau = 0.6 \text{ fm/c}$. The higher initial temperature at LHC leading to a longer fireball lifetime suggests a stronger radial flow as well as a more

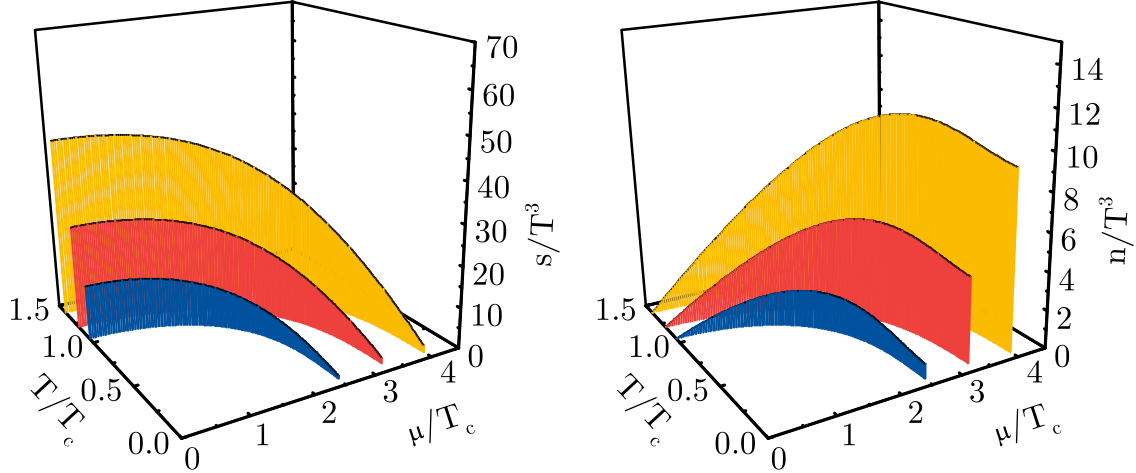


Figure 5: Scaled entropy density s/T^3 (left) and scaled net baryon density n/T^3 (right) of strongly interacting matter as predicted by the full QPM. Both quantities are exhibited along selected characteristic curves.

equilibrated azimuthal distribution of emitted hadrons. Indeed, the predicted p_T spectrum for Λ , Ξ and Ω is considerably flatter than at RHIC, while v_2 is noticeably reduced (Fig. 4).

In these examples the effects of a non-zero baryon density are negligibly small.

4 Nonzero net baryon density

The advantage of the phenomenological QPM is its ability to provide an EOS at nonzero chemical potential, in particular in a region which is expected to be relevant for forthcoming experiments at FAIR. This remarkable ability is due to the thermodynamic self-consistency of the QPM. As a consequence, thermodynamic quantities at arbitrary values of the state variables (here μ and T) are connected through Maxwell relations and the stationarity condition of the thermodynamic potential. Thus the model is able to map the lattice data at $\mu = 0$ into the T - μ -plane. This is achieved by solving the Maxwell relation, which is a partial differential equation of first order for the effective coupling $G^2(T, \mu)$, using the method of characteristics with the parametrized $G^2(T, \mu = 0)$ as initial condition. This procedure has been tested successfully against lattice calculations of the pressure corrections coefficients available for small chemical potential [11, 15].

However, the eQP, where damping terms and collective modes are neglected, meets some ambiguity in the region of large chemical potential and not too high temperatures, since the characteristic curves of the partial differential equation exhibit crossings. Consequently, for mapping to large net baryon densities the full QPM has to be applied. As a sign of the self-consistency of the latter one, no crossings appear among its characteristics [16]. Thus, the effective coupling G^2 is unique for every point of the T - μ -plane. From the effective coupling $G^2(T, \mu)$ entropy density s and net quark number density n follow directly as thermodynamic integrals. However, to ensure the physical relevance of the solutions, agreement with general thermodynamic requirements, e.g. Nernst's theorem, has to be verified.

Indeed, Fig. 5, which shows both quantities along selected characteristics starting above T_c , confirms that the entropy density vanishes for $T \rightarrow 0$ and the net number density increases with the chemical potential. Contour plots of the thermodynamic quantities (Fig. 6) also show regular behavior of the thermodynamic quantities for the region above the expected phase transition. Therefore, the full QPM can be used to predict a physical EOS for strongly interacting matter especially at high net baryon densities.

Below the “phase transition”, the model, in the present version, cannot directly be applied since strong

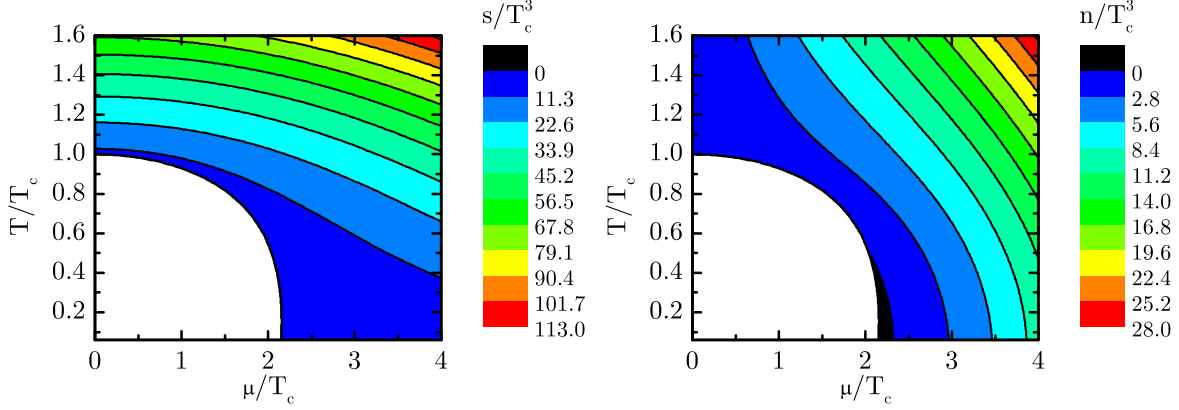


Figure 6: Contour plot of the scaled entropy density s/T^3 (left) and scaled net baryon density n/T^3 (right) as a function of temperature T and chemical potential μ from Fig. 5.

contributions of collective modes lead to a negative baryon density. It remains to be checked whether improved dispersion relations and a refined treatment of the imaginary parts of the self-energies can cure this obstacle. However, for most cases it is more prudent to use the resonance gas below the phase transition as shown for the eQP, so that these ambiguities do not pose a serious problem. The resulting “compound EOS” can then not only be used for predictions of upcoming experiments at CBM@FAIR but also as an input to general relativistic models of compact stellar objects such as neutron/quark/strange stars.

5 Conclusion

Our quasiparticle model in both the previous simplified version and the extended version with collective modes and Landau damping is able to simultaneously describe recent lattice calculations at zero and small chemical potential. Employing the resulting equation of state, combined with a resonance gas model, in a hydrodynamical code the experimental data from RHIC are fairly well described. Furthermore, predictions for heavy-ion experiments at LHC can be given. For both experimental situations the simplified, effective quasiparticle model suffices due to small net baryon densities. However, for larger net baryon densities, the full model including the suitably parametrized HTL dispersion relations, Landau damping and collective modes has to be employed. The current results are encouraging with respect of deriving an equation of state usable in a large region of the phase diagram of strongly interacting matter.

Acknowledgment: R.S. would like to thank the organizers for the invitation to this very insightful and inspiring meeting and the financial support granted.

References

- [1] J. Kapusta, B. Müller, J. Rafelski, *Quark-Gluon Plasma: Theoretical Foundations* (Elsevier, 2003), ISBN 0444511105
- [2] I. Arsene et al. (BRAHMS), Nucl. Phys. A **757**, 1 (2005), [nucl-ex/0410020](#)
- [3] B.B. Back et al. (PHOBOS), Nucl. Phys. A **757**, 28 (2005), [nucl-ex/0410022](#)
- [4] J. Adams et al. (STAR), Nucl. Phys. A **757**, 102 (2005), [nucl-ex/0501009](#)
- [5] K. Adcox et al. (PHENIX), Nucl. Phys. A **757**, 184 (2005), [nucl-ex/0410003](#)

- [6] A. Peshier, B. Kämpfer, O.P. Pavlenko, G. Soff, Phys. Lett. B **337**, 235 (1994)
- [7] A. Peshier, B. Kämpfer, O.P. Pavlenko, G. Soff, Phys. Rev. D **54**(3), 2399 (1996)
- [8] P. Lévai, U. Heinz, Phys. Rev. C **57**, 1879 (1998), [hep-ph/9710463](#)
- [9] A. Peshier, B. Kämpfer, G. Soff, Phys. Rev. C **61**, 045203 (2000), [hep-ph/9911474](#)
- [10] A. Peshier, B. Kämpfer, G. Soff, Phys. Rev. D **66**, 094003 (2002), [hep-ph/0206229](#)
- [11] M. Bluhm, B. Kämpfer, G. Soff, Phys. Lett. B **620**, 131 (2005), [hep-ph/0411106](#)
- [12] B. Kämpfer, M. Bluhm, R. Schulze, D. Seipt, U. Heinz, Nucl. Phys. A **774**, 757 (2006), [hep-ph/0509146](#)
- [13] M. Bluhm, B. Kämpfer, R. Schulze, D. Seipt, Acta Phys. Hung. A **27**, 397 (2006), [hep-ph/0608052](#)
- [14] M. Bluhm, B. Kämpfer, R. Schulze, D. Seipt, Eur. Phys. J. C **49**, 205 (2007), [hep-ph/0608053](#)
- [15] M. Bluhm, B. Kämpfer, R. Schulze, D. Seipt, U. Heinz, Phys. Rev. C **76**, 034901 (2007), [arXiv:0705.0397](#)
- [16] R. Schulze, M. Bluhm, B. Kämpfer, Eur. Phys. J. ST (2008), in print, [arXiv:0709.2262](#)
- [17] J. Letessier, J. Rafelski, Phys. Rev. C **67**, 031902 (2003), [hep-ph/0301099](#)
- [18] M.A. Thaler, R.A. Schneider, W. Weise, Phys. Rev. C **69**, 035210 (2004), [hep-ph/0310251](#)
- [19] J.M. Cornwall, R. Jackiw, E. Tomboulis, Phys. Rev. D **10**, 2428 (1974)
- [20] M.L. Bellac, *Thermal Field Theory* (Cambridge University Press, 1996), ISBN 0521654777
- [21] F. Karsch (2007), [hep-ph/0701210](#)
- [22] F. Karsch, K. Redlich, A. Tawfik, Phys. Lett. B **571**, 67 (2003), [hep-ph/0306208](#)
- [23] C. Bernard et al., PoS **LAT2005**, 156 (2006), [hep-lat/0509053](#)
- [24] Y. Aoki, Z. Fodor, S.D. Katz, K.K. Szabó, JHEP **2006**, 089 (2006), [hep-lat/0510084](#)
- [25] J. Adams et al. (STAR Collaboration), Phys. Rev. Lett. **95**, 152301 (2005), [nucl-ex/0501016](#)